JOURNAL OF MATERIALS SCIENCE 20 (1985) 4465–4478

Gel-drawn fibres of poly(vinyl alcohol)

PEGGY CEBE*, DAVID GRUBB
Department of Materials Science and Engineering, Cornell University, Ithaca, New York 14853, USA

Semi-crystalline gels of several samples of poly(vinyl alcohol) were made from solutions in which the polymer concentration varied from 2.0 to 15.0%. Entanglement density in the material was in this way reduced from the melt entanglement density. When gels were partially dried and drawn isothermally the maximum draw ratio increased with drawing temperature up to 11 to 14 at 140 to 180° C. A melt-cast film could be drawn to 6.8 times at 140° C. Drawn material had a crystallinity of 55 to 80%, while that of isotropic material was 20 to 55%. Gels of lower initial concentration (lower entanglement density) could be drawn to greater extensions at a given draw temperature and had better mechanical properties. Young's modulus increased with draw ratio to values very close to those for polyethylene fibres drawn by the same amount. Young's modulus was independent of drawing temperature or degree of crystallinity, but on comparing drawn gels of the same draw ratio, crystallinity and crystalline orientation, those of lower entanglement density had a higher Young's modulus.

1. Introduction

Published work on the production of high-modulus fibres from flexible linear polymers has been largely concerned with polyethylene (PE), and one reason for this is the high Young's modulus along the chain axis, of 250 to 300 GPa [1, 2]. (For a recent review of all such work, see Ohta [3].) Ultra-high values of fibre tensile modulus in PE (over 50 GPa) were first achieved by hot-drawing melt-crystallized material [4–6]. It was found that the modulus was a monotonically increasing function of draw ratio λ, and that other processing variables had much smaller effects than λ [5, 6]. Thus, if a method could be found to draw any given starting material to high λ, the result should be a high-modulus fibre (unless the temperature is too high and the molecules can relax so that the process is only the extensional flow of a liquid).

Some authors [7–9] have formed high-modulus PE fibres from dilute solutions of high molecular weight polymer at the surface of a rapidly spinning rotor. Smith and co-workers [10–13] have obtained high-modulus fibres (E = 90 to 100 GPa) by drawing PE gels. Gels were made from solutions of a range of initial concentrations, C. High-modulus fibres having high draw ratios were obtained from high molecular weight material when the initial solution concentration was low, even if the gels were completely dried before drawing. The maximum value of λ obtainable under given conditions, λ_{max}, was found to be proportional to $C^{-1/2}$, just as predicted from the extensibility of the entanglement network [13]. Smith and Lemstra concluded that the entanglement density in solution, reduced to $\xi_e' = C\xi_e$ from its melt value ξ_e, is preserved in the gel and controls drawing behaviour [13]. The moduli of drawn gels show trends similar to those of other drawn PE fibres. In particular, the modulus depends primarily on λ and all other variables such as draw temperature, molecular weight and sample history (initial solution concentration or thermal treatment) are much less important [14].

Further work on fibres grown from dilute

Present address: Jet Propulsion Laboratory, Pasadena, CA 91109, USA.

0022–2461/85 $03.00 + .12

solutions and drawn from gels has established a connection between the formation of high-modulus fibres at high temperature by the surface growth technique and the presence of surface-adsorbed layers which can form gels [15]. Such fibres, although prepared from a mobile dilute solution, can thus be described as stretched gels. It has also been shown that shish-kebab crystals, typically seen to form in stirred dilute solutions, are an intermediate state in gel drawing [16]. Single crystals formed from quiescent dilute solution should have a very low entanglement density, and mats of single crystals have been drawn to $\lambda > 300$, forming high-modulus fibres [17]. When a single-crystal mat is melted the melt viscosity is very low, and it increases to a normal value over a period of time [18]. This is direct evidence for the reduction in ξ_e by solution processing, and the gradual re-establishment of the equilibrium value in the melt.

Conditions for successful drawing of melt-crystallized material to high λ are the same as those for disentanglement during drawing, that is, slow drawing at high temperature of material of moderate molecular weight [4–6]. Achievement of high draw ratio can then by itself be taken as evidence for reduced entanglement density ξ_e' [19], and ξ_e' is the common feature in high-modulus fibres from PE, controlling λ and thus the modulus.

To get high-modulus fibres from other polymers we should look for high draw ratios and reduced entanglement densities, and gelation is the best controlled way to reduce entanglement density. Peguy and Manley [20] have used this route for polypropylene, drawing dried gels [21] originally formed at 1% polymer concentration to $\lambda = 57$. The resultant fibres have nearly the theoretical modulus and strength of polypropylene, but the helical conformation of the molecules in the crystal makes this theoretical modulus much less than that of PE at only 41 GPa [22]. The "other polymer" considered here is poly(vinyl alcohol) (PVA), chemically a near relative of PE. PVA has an all-*trans* chain conformation in the crystal and a crystal structure very similar to that of PE, so the theoretical Young's modulus in the chain direction is very high. It also has high crystal relaxation and melting temperatures compared to PE, so that a higher temperature of use and better creep resistance may be expected. For comparison the crystalline relaxation occurs at 140° C in PVA and 70° C in PE, while crystals melt at 240° C in PVA and 140° C in PE. The transition temperatures in PVA are so much higher because of the strong polar interaction between the chains.

Strong interaction between chains is expected to make the drawing behaviour very different to that of PE, and the polar hydroxyl groups also cause the material to be sensitive to water. The crystalline homopolymer PVA does not dissolve in water except at high temperature, but just as for polyamides, the mechanical properties are strongly affected by water absorption. Several groups have investigated the gelation of PVA from various solvents [23–27] and Yamaura and co-workers [28–30] have studied crystallization from stirred solution and gelation as a function of the chemical structure of the PVA (molecular weight, residual ester group content and distribution, branching, tactivity and head-to-head content). Kwon, Kavesh and Prevorsek have recently shown in a patent disclosure [31] that PVA of molecular weight over 500 000 and preferably $\approx 2 \times 10^6$ can be processed by gel spinning, drying and drawing in two or three stages to give fibres of modulus up to 70 GPa and strength up to 2 GPa. The total draw ratio they used was 10 to 20 ×. Here we present the results of a study of isothermal gel drawing of lower molecular weight PVA.

2. Experimental details

2.1. Fibre production

The starting materials used were of two types: PVA powders nominally 99 to 100% hydrolysed and of weight-average molecular weights 115 000 and 86 000 (Scientific Polymer Products, Inc., Ontario, New York), and high-tenacity PVA fibres kindly supplied by Kuraray Co. and by P. J. Lemstra. Gels formed from these materials were named D, F, K and L during this study. Viscometry of the four samples in a 1 : 3 mixture of ethylene glycol and water at 35° C showed that the molecular weights of the K and L fibre samples lay between those of the powders and were approximately 93 000 and 87 000 respectively. Infrared (IR) and nuclear magnetic resonance (NMR) analysis showed that all the materials were essentially atactic.

PVA powder was dissolved in a 2 : 1 mixture

of ethylene glycol and water at 135° C. After a few hours the hot solution was poured on to a glass tray where it gelled on cooling. The fibres could not be dissolved in this way, so they were dissolved in pure ethylene glycol at 195° C. The temperature of the solution was lowered to just below 100° C and water added to give the required 2 : 1 ratio. After homogenizing the solution at 135° C it was gelled in a glass tray as before. At room temperature syneresis occurred for several days. The drying process was then continued by heating to 60° C in a vacuum oven. When dry, gels were transparent, brittle and difficult to handle. Dried gels were cut from the glass and allowed to absorb a little water before being pushed into tensile specimens with a gauge length of 0.5 in. (12.7 mm). These specimens were drawn without re-drying at elevated temperatures in an Instron tensile tester at 10 in. min^{-1} (254 mm min^{-1}). Extension was measured from the separation of marks on the gauge section for samples that were not taken to failure. Extension of samples that were drawn to break was obtained from crosshead movement.

2.2. Fibre characterization

After drawing, the centre of the gauge section was cut out and dried in methanol at room temperature to remove the residual solvent, which was about 17% by weight of the drawn fibre. The stress–strain curves of the dried, drawn gels were obtained at room temperature using a crosshead speed of 0.005 in. min^{-1} (0.13 mm min^{-1}). This mechanical test was not performed in a controlled atmosphere so re-absorption of water is likely. Young's modulus was calculated from the slope of the curve in the region below 0.3% strain.

Thermal analysis was performed using a Perkin–Elmer DSC–2C. Crystallinities were calculated from the area of the fusion peak using 156.2 J g^{-1} as the heat of fusion of PVA crystals [32]. Drawn samples were tested at a heating rate of 20° C min^{-1}, and were allowed to contract freely during heating. Wide- and small-angle X-ray diffraction patterns were obtained using flat-plate geometry and a Statton camera. Fibre orientation of crystalline PVA in the drawn samples was estimated from the angular spread of the (1 1 0) reflection.

Optical microscopy with a Mettler hot stage was used to examine the retraction of the drawn gels upon heating near the melting point. Two testing procedures involving different sample histories were used to distinguish the effects of heating rate on retraction. To get the retraction as a function of temperature at a fast heating rate, many pieces were cut from a single fibre and each was placed in the hot stage when it was equilibrated at the required temperature. In the slow heating test, a single fibre was heated from room temperature to the melting point, and its length was continuously measured. Shrinkage was described as a retraction R defined as [33]

$$R = (L_d - L_s)/(L_d - L_0)$$

where the sample length is L_0 before drawing, L_d after drawing, and L_s after shrinking. L_0 was not measured but calculated as L_d/λ, giving

$$R = \frac{1 - L_s/L_d}{1 - 1/\lambda}$$

3. Results and discussion

3.1. Drawing of PVA gels

Typical stress–strain curves obtained during hot drawing are shown in Fig. 1. Fig. 1a contains curves obtained from gels made from PVA powder of molecular weight 115 000 (D-gels) at a range of concentrations and drawn at the same temperature. Fig. 1b contains curves obtained from L-gels of initial concentration 4.2% drawn at a range of temperatures. Fig. 1a shows that yield stress and neck formation are relatively insensitive to the initial concentration of the gel, but the orientational hardening and thus the stress at high strains increases with concentration. The apparent reversal of this trend at 15% concentration is due to slippage at the grips. Higher concentration gels were thicker and difficult to grip at the high temperatures of drawing. Fig. 1b shows that both the yield stress and the rate of strain hardening decrease as the drawing temperature increases. The failure at $\lambda = 7$, $T_d = 168°$ C seems premature and may be due to surface defects. To get very high draw ratios, the drawing stress should remain fairly constant [11] so that Fig. 1b shows that a high drawing temperature will be required.

In Fig. 2a the maximum draw ratio λ_{max} is plotted as a function of the drawing temperature for various concentrations of D-gels. In this series of tests all samples were drawn to failure, so λ_{max} was calculated from the crosshead movement.

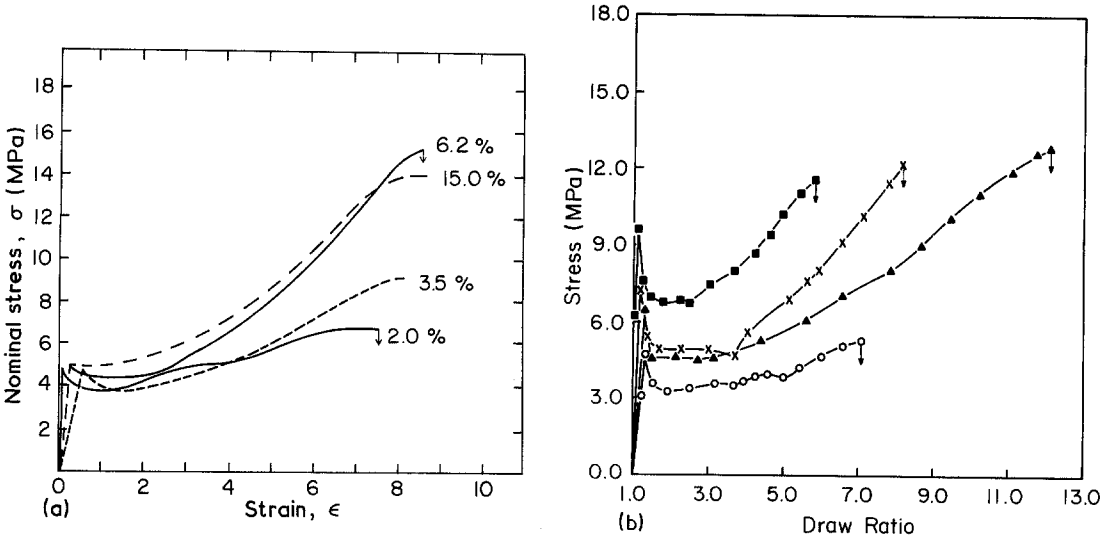

Figure 1 (a) Stress–strain curves produced during hot drawing of different concentration D-gels (molecular weight 115 000, powder). Drawing temperature is in the range 111° to 115° C. Arrows indicate sample fracture. Tests for 3.5% and 15% gels were stopped before fracture. (b) Stress–strain curves produced during hot drawing of L2, an L-gel of 4.2% concentration, at various temperatures. Arrows indicate sample failure. Values of T_d: (■) 85°, (x) 111°, (▲) 138°, (○) 168° C.

λ_{max} represents an average over the entire drawn portion of the fibre, and this includes the less highly drawn material adjacent to the grips. When values of λ_{max} were compared to the extension of the highly drawn central region of unbroken samples, λ_{max} was 5 to 10% smaller. Thus λ_{max} is a lower limit to the extension of the fibre during drawing, and when higher λ values are quoted later, they refer to the highly drawn central portions. λ_{max} goes through a plateau

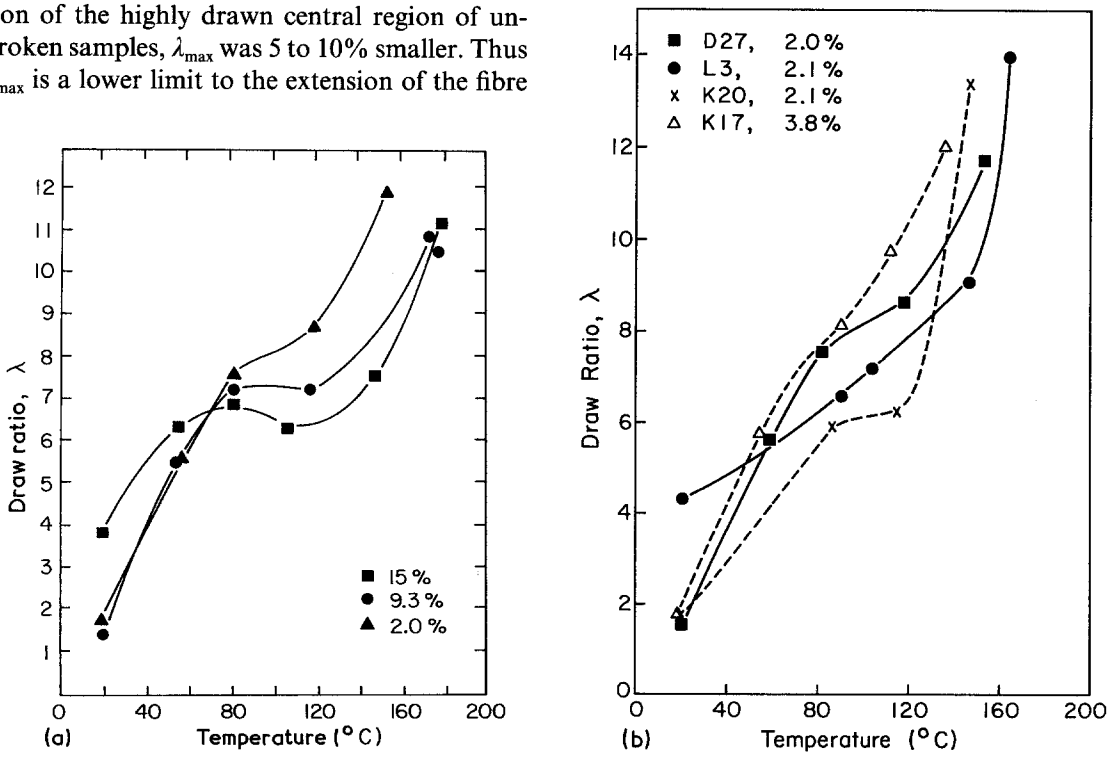

Figure 2 (a) Draw ratio as a function of drawing temperature for different concentration D-gels. The draw ratio plotted is the maximum value attained after many trials at each temperature. (b) Draw ratio as a function of drawing temperature for low-concentration gels produced from different starting materials. As in Fig. 2a, the draw ratio plotted is the maximum value obtained.

near the glass transition temperature (86° C), then increases as the temperature approaches the crystal relaxation temperature (140° C). The anomalous behaviour of the 15% gel, which draws to nearly four times at room temperature, is due to solvent retention. This sounds odd, for the gels of *low* concentration contain much more solvent to begin with. However, the casting of a low-concentration gel results in a thinner film after drying so that by the time a film originally 2% has dried to 15% solids concentration, it is much thinner than we can cast a 15% gel. It thus continues to dry at a faster rate. The plasticization of the 15% gel will reduce the glass transition temperature so that the plateau in λ_{max} will also be reduced in temperature. However, as the temperature rises, solvent will be extracted from the sample during temperature equilibration and drawing, particularly as the heating is by forced hot air. At higher temperatures of drawing the solvent effect is reduced and the trend shown is for the higher draw ratios to be achieved with lower concentration samples. Similar plots of λ_{max} against drawing temperature for some gels made from fibre starting materials are shown in Fig. 2b. In most cases λ_{max} increases continuously with drawing temperature, with a slight plateau in evidence for the K-gels of concentration 2.1%.

When gels were drawn at 180° C, the maximum draw ratio obtained from high-concentration gels increased, but only to $\lambda = 12$. The fibres formed in this way had very low Young's modulus (1 to 3 GPa) indicating that the molecules were relaxing during drawing, or possibly that chemical degradation of PVA was affecting the properties. Two of the L-gels, with concentration 2.4 and 4.2%, had a peak in λ_{max} (at about 140° C) and a significant decrease, to less than 10, at the highest temperatures. These are not shown in Fig. 2b, but the L-gel of concentration 4.2% is shown to fail at low λ in Fig. 1b. Similar behaviour was seen by Smith and Lemstra [34] in gels of PE and attributed to the effect of residual solvent. These L-gels had a slightly higher than normal extension at room temperature and a longer region of strain hardening before failure which indicates plasticization, but the 15% gel (Fig. 2a) which is clearly platicized does not show the same effect. The premature failure of these particular L-gel samples at high temperatures may have been due to a high concentration of surface defects.

TABLE I Physical properties of gels

Concentration (%)	l'_e (nm)	d' (nm)	λ_{th}	λ_{max}
100.0	14.0	4.65	1.7	6.8
15.0	93.3	12.0	4.5	11.3 (at 180° C)
9.3	151	15.2	5.7	11.0
6.2	226	18.7	7.0	12.2 (at 180° C
4.2	333	22.7	8.5	12.0
3.8	369	23.9	8.9	12.0
2.4	584	30.0	11.2	12.2
2.0	701	32.9	12.3	14.0

In Table I, maximum theoretical and experimental draw ratios are listed for all the gel concentrations used in this study along with values for l'_e and d', where l'_e and d' are the chain contour length between entanglements and the rms distance between entanglements, respectively. The theoretical draw ratio of a three-dimensional network is given by

$$\lambda_{th} = l'_e/(3^{1/2}d')$$

The factor of $3^{-1/2}$ comes from consideration of the average projection of the network strand on the tensile axis. In a gel formed from a solution of polymer volume fraction C, $l'_e = l_e/C$ and $d' = d/C^{1/2}$ where l_e and d relate to the "undiluted" network which exists in a melt. In PVA, $l_e = 14$ nm and $d = 4.65$ nm. These numbers are derived from a molecular weight between entanglements of 2400 [32] and a ratio between end-to-end distance and molecular weight of 0.095 nm (amu)$^{-1/2}$. For gels drawn at temperatures above 140° C, experimental draw ratios range from 11 to 14. In all cases the draw ratios observed are larger than those predicted by the theory of entanglement-limited drawing, but the range observed is very narrow compared to the range of 1.7 to 12 for λ_{th}. The last two rows in Table I show the critical overlap concentration c^* for the extreme values of molecular weight used here. At c^* the molecules are only just entangled, and drawing to λ_{th} from c^* would fully stretch out the molecules. At concentrations less than c^*, cooling the solutions should lead to suspensions and not gels, and no gels could be formed from solutions of concentration less than 2%. If there are only weak intermolecular interactions then drawing to extensions greater than the λ_{th} derived from c^* should lead to loss of strands from the network

and loss of strength. The limiting draw ratio of Table I could be due to this limitation of the material, as disentanglement at high draw ratios could lead to strand loss, weakness and failure even in gels formed well above c^*. In that case, an increase in molecular weight would allow higher draw ratios. Alternatively, there could be a limitation imposed by the drawing system.

As published work on gel drawing relates chiefly to PE it is clear that the behaviour of PVA should first be compared with that of PE. The trends shown in Fig. 1 are very similar to those of PE, that lower initial gel concentrations and higher draw temperatures give rise to flatter stress–strain curves [13] (less strain hardening), and higher draw ratios with a few exceptions discussed above. However, the PE gels could be drawn to much higher λ_{max} [34] and the variation of λ with concentration was much closer to that predicted theoretically. Often in PE gel drawing the λ_{th} used is just l'_e/d' without the $3^{-1/2}$ geometric factor. This is because at temperatures just above the crystal relaxation temperature of 70° C both the solid melt-crystallized material and gels of all concentrations could be drawn to l'_e/d'. In PVA, l'_e/d' is 15 to 20 for concentrations of 4 to 2%, so few of the low-concentration gels reached l'_e/d'. In PE, drawing at high temperatures can give a much higher λ. For example the melt-crystallized material can be drawn to 40 times [4–6], gels have been drawn up to 100 times [35], and single-crystal mats up to 350 times [17]. The $3^{-1/2}$ factor is not very important since neither formula takes account of strand-length distribution or entanglement-point slippage, or any of modern network theory. It is mentioned because its use here could lead one to believe that PVA and PE entanglement densities are more different than they are. λ_{th} for PE has been given as 3.7 [13]; when calculated on the same basis λ_{th} for PVA is 3.0, not 1.8 as in Table I.

Several reasons present themselves for the reduced maximum drawability of the PVA gels in this study:

(a) Inter-chain bonding in PVA is by relatively strong hydrogen bonding, and this may inhibit mobility during drawing even at temperatures above the crystal relaxation temperature. The chains will then not be able to disentangle during drawing and λ will be limited to λ_{th} or less if the molecular chains cannot move easily through the crystals.

(b) All the very highest values of λ in PE have been obtained with high molecular weight material where c^* is low, and the draw ratio to fully extend the molecular chains is not much exceeded. Thus the starting materials used here may simply be of too low a molecular weight for ultra-high draw ratios.

(c) The drawing oven required some equilibration after a sample was inserted, so that each sample had 6 to 8 min at high temperature before drawing. This may have allowed some re-entanglement, which would tend to reduce differences between initial concentrations and to reduce λ. It did allow relaxation of the gel within the grips, and slippage at high temperature was common.

We know that (a) is not an absolute limitation of the material because samples of high initial entanglement concentration can be drawn to high λ, producing fibres of good mechanical properties by the process of zone drawing, where the sample sees a very high temperature for a very short time [3, 36–38]. Reason (b) is not wholly convincing because PE of molecular weight 100 000 can be drawn to 35 times [3, 4], which is about 30% over l'_e/d' or 60% over λ_{th}. If PVA of the same molecular weight could be drawn to the same amount, we would have λ_{max} of 25. The *gel* drawing of PE, however, has only been reported with much higher molecular weight material. The practical problems of (c) would be eliminated by zone drawing.

3.2. Fibre characterization

Since the purpose of fibre production is to get stiff and strong material, and only the crystalline phase is stiff, it is important to know the crystallinity of the fibres and how this varies with preparation parameters. Total crystallinity was obtained from the area under the melting endotherm in the differential scanning calorimeter (DSC), so there is no distinction made between different forms of crystal, i.e. lamellar or fibrillar or different arrangements of crystals. In PE fibres the Young's modulus varies while the total crystallinity remains roughly constant, and the increase of Young's modulus is explained by a change from mechanically isolated to mechanically connected crystals (which

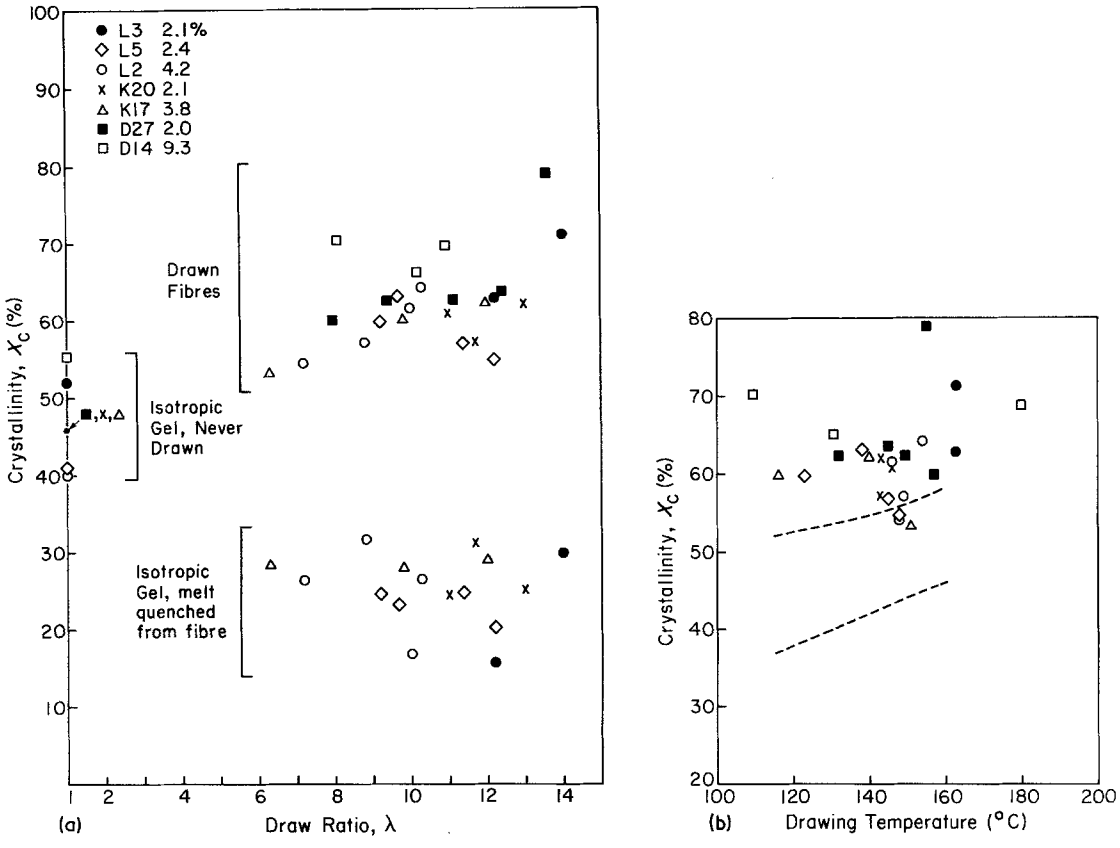

Figure 3 (a) Crystallinity plotted as a function of draw ratio. Points having a draw ratio of unity represent the isotropic gel before drawing. Crystallinities of the drawn fibres are greater than those of the isotropic gel. When the fibres are melted, the isotropic samples that result have greatly reduced crystallinities. D-series fibres degraded during melting and were not retested. (b) Crystallinity plotted as a function of drawing temperature for drawn fibres. The dashed lines represent the upper and lower bounds on crystallinity induced by annealing in the same temperature range.

may or may not be physically connected into larger crystals) [4, 19, 39, 40]. A change from lamellar to fibrillar crystals [7, 8] will have a similar mechanical effect. Nevertheless, measurement of total crystallinity is an important first step in modelling the modulus.

After drawing gels of PVA the melting endotherms became much narrower and melting points increased by an average of 6.5° C, indicating that more-perfect crystals are formed during drawing. Total crystallinity is plotted against λ in Fig. 3a for three sets of samples. Isotropic undrawn dried gels have crystallinities ranging from 40 to 55%. The range in drawn samples made from the same starting material is 53 to 79%. After the drawn fibres had been melted in the DSC they were quenched to room temperature and retested. The crystallinity of this melt-quenched material is much less than that of the original gels, and also much less than that of the material in their as-received state, powder or fibre (Fig. 3a). It is not surprising that rapid cooling in the presence of solvent to form the gel allows more molecular motion than rapid cooling from the melt in the absence of solvent, so that greater crystallinity can develop. This greater mobility will not persist at low temperature when crystals have formed, so that the solution entanglement density can still be permanently "frozen in" in the gel at room temperature.

In Fig. 3a the crystallinity of the drawn fibre shows almost no variation with λ. A slight tendency for crystallinity to increase with λ is supported mainly by the two samples with the largest values of crystallinity and λ. There is no pattern of variation for the crystallinity of samples formed by quenching gels, nor does the crystallinity of the original unoriented gel seem to have any effect. This indicates that chemical

TABLE II Effects of annealing gels

T_a (° C)	Gel number and concentration (%)						
	D17	D27	C17	C20	L2	L5	L3
	9.3	2.0	3.8	2.0	4.2	2.4	2.1
Crystallinity (%)							
No anneal	42	46	46	46	40	41	52
115	43	50	46	49	37	48	52
145	43	50	47	50	44	49	55
160	58	50	56	52	46	50	55
Melting point (° C)							
No anneal	230	227	229	229	229	228	230
115	229.5	227	229	229	229	229	230
145	230	227	229	229	229	230	230
160	230	227	229.5	230	230	230	230

differences in the starting materials and chemical degradation during drawing are not important, at least for crystallinity.

The effect of drawing temperature T_d on crystallinity is shown in Fig. 3b. Annealing experiments were performed in the same temperature and time regime as hot drawing, to determine whether crystallinity changes could be attributed to thermal effects alone. Undrawn gel samples were heated in the DSC to the annealing temperature and held for 10 min, then cooled and tested. Results for crystallinity and melting point of annealed gels are shown in Table II. Melting points of the annealed gels are very close to those of the unannealed gels. Crystallinities showed a definite increase as the annealing temperature increased. Lower-concentration gels experience the greatest change in crystallinity at 115° C, the lowest annealing temperature. Higher temperature causes little further change in crystallinity for the low-concentration gels. In contrast, the high-concentration gels do not change in crystallinity until the temperature is much higher, and nearly all the increase occurs at 160° C. This dependence on concentration gives a range of crystallinities obtained by annealing which is shown by the lines in Fig. 3b.

All of the drawn samples have crystallinities (X_c) greater than that obtainable by annealing (Table III). (The three points which fall between the lines in Fig. 3b all have crystallinities greater than that of their annealed counterparts, as can be verified from Table II.) We conclude that hot drawing improves the crystallinity of the material to a greater extent than simple annealing does. Annealing also has less effect on crystal perfection, since the melting point hardly increases on annealing, but increases very significantly on drawing as shown in Table III. Shrinkage results to be described below show that the increase in melting point is not due to superheating or constraints on the fibre.

Plots of Young's modulus against λ are given in Fig. 4 for a range of gel concentrations, from data in Table III. When all the data are included (Fig. 4a), the plot contains a broad band of points with a clearly positive slope. One reason for the large scatter in E is the formation of voids during drawing. Stress-induced whitening was clearly visible when samples were drawn at low temperature, and optical microscopy of samples drawn at 140° C indicated the presence of elongated voids not present before drawing. Inter-chain bonding in PVA is strong even at high temperatures, as is shown by the lack of disentanglement during drawing and the small reduction in drawing stress when the drawing temperature is increased from 111 to 168° C (Fig. 1b).

Restricting the data set to draw temperatures from 140 to 165° C and to gel concentrations less than 5% gives Fig. 4b, a much more well-defined dependence of Young's modulus on λ. Included in Fig. 4b are six points for drawn melt-crystallized PE taken from the literature [6]. They are there purely for comparison. They show that ultra-high values of the Young's modulus are not to be expected at these limited draw ratios. The observed maximum value of 20 GPa is a respectable figure for a polymer fibre; it is close to the Young's modulus of commercial PVA tyre cord (Kuraray Co.), but it is

TABLE III Effects of drawing gels

Sample	Concentration (%)	λ	T_d (°C)	T_m (°C)	X_c (%)	E (GPa)
D27	2.0	1.0	–	229	46	–
		8.0	157	236.5	60	9.4
		9.4	132	236	62	6.0
		11.0	152	235	61	10.1
		12.4	145	235	64	15.1
		13.6	155	235	79	19.9
C17	3.8	1.0	–	229	46	–
		6.3	151	236.5	53	4.7
		9.8	116	237	60	8.4
		12.0	140	237	62	10.5
C20	2.1	1.0	–	229	46	–
		11.0	146	235	61	10.9
		11.7	143	234	57	13.1
		13.0	143	237	62	12.6
L2	4.2	1.0	–	230	52	–
		7.2	148	237.5	54	5.2
		8.8	149	237	57	5.3
		10.0	146	237	62	8.6
		10.3	154	239.5	64	7.1
L5	2.4	1.0	–	228	41	–
		9.2	123	237	60	11.3
		9.7	138	237	63	10.1
		11.4	145	236.5	57	8.2
		12.2	148	236	55	11.8
L3	2.1	1.0	–	230	52	–
		12.2	163	237	63	12.4
		14.0	163	237.5	71	17.2

less than 10% of the theoretical crystal Young's modulus for PVA.

Fig. 4b also makes it clear that the data so far obtained are insufficient to prove or disprove the suggestion that the modulus of all entanglement-limited drawn fibres will give a straight line if plotted as $1/E$ against $1/\lambda^2$ [19]. This plot can only be superior to the direct plot of E against λ if the direct plot gives a curve that is sigmoidal in shape, levelling off at very high modulus as some saturation value is approached. The curve in Fig. 4b is still increasing in slope at the draw ratios accessible, and the same is true for PE data at $\lambda < 25$.

Fig. 5 is a direct check on the correlation between crystallinity and Young's modulus. Crystallinity lies in the range 53 to 65% while Young's modulus varies widely from 4.7 to 15 GPa. There is essentially no dependence of E on λ for the PVA gels, although the very highest moduli were obtained at the highest crystallinities. As in Fig. 3a, two fibres stand out, that made from an L-gel of 2.1% concentration with $\lambda = 12.0$ and that from a D-gel of 2.0% with $\lambda = 13.6$. Without these one would say that there is no relation between crystallinity and λ or between crystallinity and Young's modulus. With these fibres of the highest observed λ, there is some indication that crystallinity may begin to change at higher draw ratios.

Fig. 5 can also be used to make general comparisons between the various starting materials. All 4.2% L-gels have moduli below 8.4 GPa, the 2.4% gels have moduli in the range 8.1 to 1.8 GPa, and the 2.1% L-gels have the highest moduli of 12.4 to 17.2 GPa. Considering the K-gels in the same way, at 3.8% the modulus range is 4.7 to 10.5 GPa, but the lower-concentration 2.1% gels are in a higher range at 10.9 to 13.1 GPa. It would seem clear that Young's modulus increases as initial concentration decreases. A closer look shows that the reason for this trend is that the lower-concentration materials can be drawn to higher λs and this gives a higher modulus. If we were to take the same modulus data as presented in

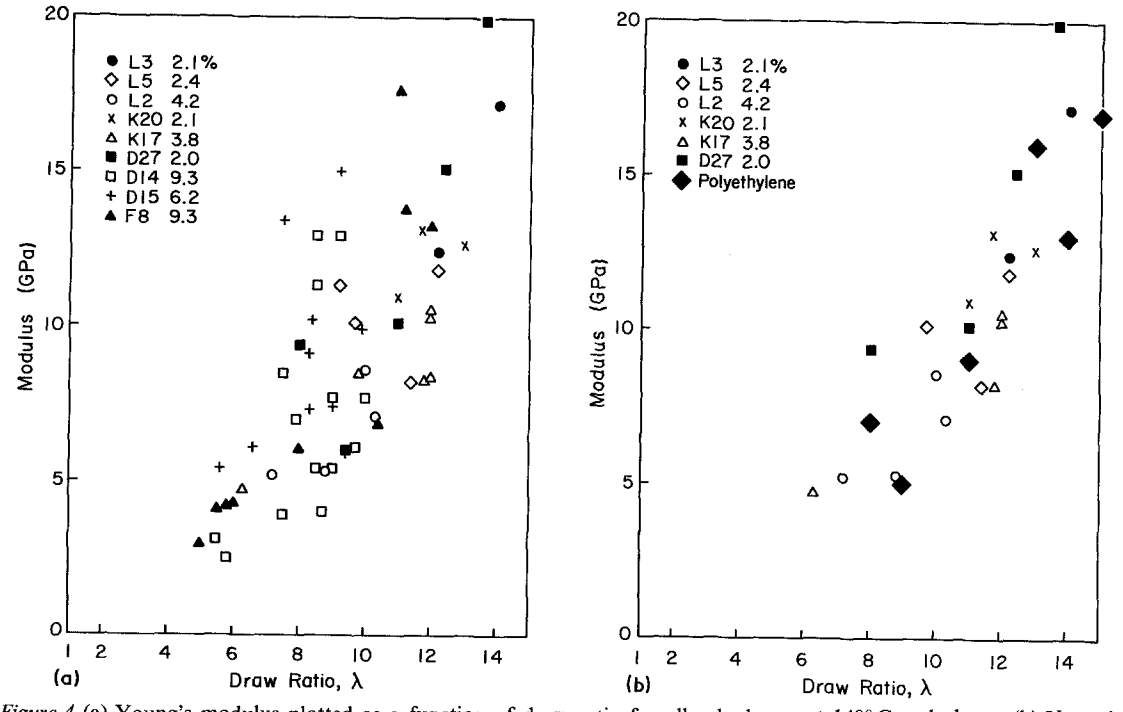

Figure 4 (a) Young's modulus plotted as a function of draw ratio for all gels drawn at 140° C and above. (b) Young's modulus plotted as a function of draw ratio for gels of concentration less than 5%, drawn at temperatures between 140° and 165° C. These data produce a better defined relationship. The data for polyethylene fibres (large filled diamonds) are literature values [6] for comparison.

Fig. 4a and compare different concentrations at the same λ the trend would be the opposite, *higher* concentration gels having the higher modulus. A theory of the Young's modulus of drawn gel fibres [19] has the entanglements acting as defects in the fibre, reducing the modulus so that lower concentration gels should have higher Young's modulus. However, this theory relates to the fully oriented state, which is not arrived at until the gel is drawn to λ_{th}. If fibres are compared at the same draw ratio, which produces full orientation only for gels of high concentration, the material of low concentration, not fully drawn, may well show a lower modulus.

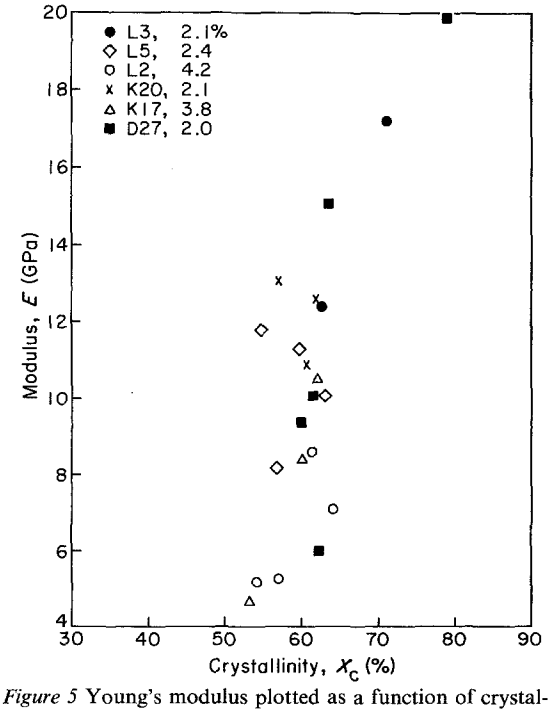

Figure 5 Young's modulus plotted as a function of crystallinity for PVA fibres drawn from gels.

Crystal orientation in the drawn fibres was measured by wide-angle X-ray diffraction using the angular range of the arc of the strong (1 1 0) reflection, and the results are shown in Fig. 6. Lines in Fig. 6a and b connect data points from gels of the same starting material and initial concentration (entanglement density). In Fig. 6a the orientation angle is plotted against draw ratio. At low draw ratio there is a large spread in orientation angle which narrows as λ increases. The orientation continues to improve substantially in the range of draw ratios covered here. In PE fibres, ultra-high modulus is not achieved until drawing proceeds at nearly perfect orientation. Fig. 6a does not show any significant

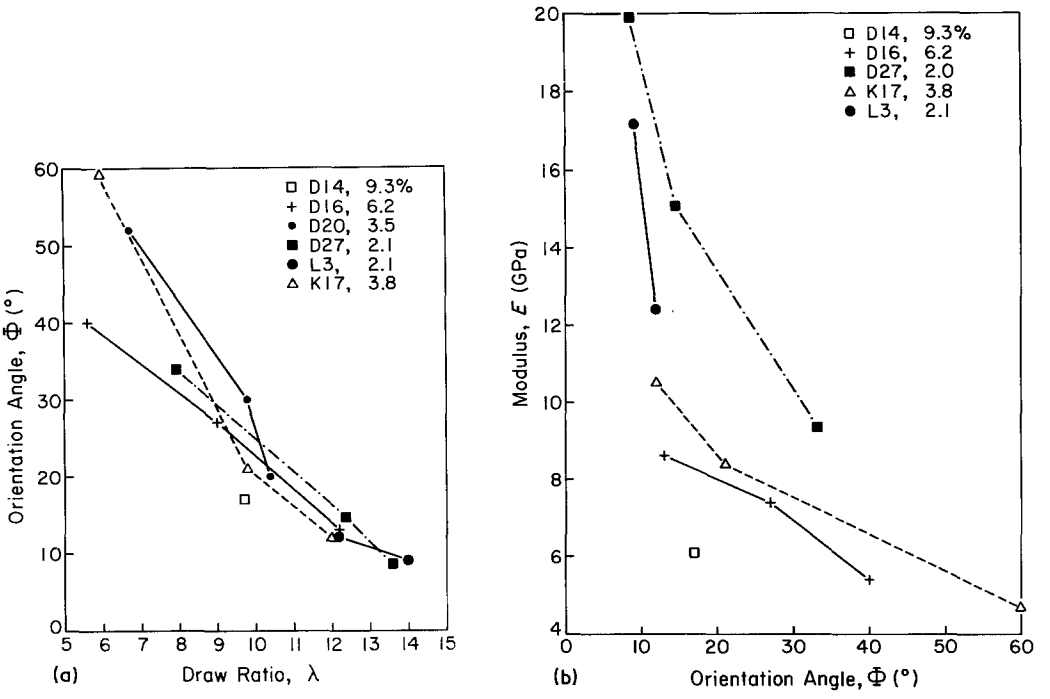

Figure 6 (a) Orientation angle Φ of the (1 1 0) reflection plotted as a function of draw ratio for fibres of PVA drawn from a number of different gels. (b) Young's modulus plotted as a function of Φ for the PVA fibres used in Fig. 6a.

difference in orientation angle between different starting materials. Fig. 6b contains the same orientation data plotted against the Young's modulus of the fibre. Now the different materials and concentrations are well separated. At a given orientation angle, fibres of lower concentration have a higher modulus. The four points in Fig. 6a at a draw ratio near to 12.2, for example, have orientation angles between 12° and 14.5°. These four points replotted in Fig. 6b are no longer together, as the moduli of these samples range from 8.5 to 15.1 GPa. Thus draw ratio is not the only factor controlling modulus. Solution concentration, i.e. entanglement density, has a direct effect in that when gels of the same draw ratio and crystalline orientation are compared, those with a reduced entanglement density have the higher Young's modulus. This is true only when all the gels are drawn to $\lambda > \lambda_{th}$ (remember that at low λ the high-concentration gels have a higher modulus) and when the orientation angle has still not reached its limit. Orientation angle is not considered an important variable in PE fibres because it is always very small, although improvements in the perfection of crystal orientation are still seen at extremely high draw ratios [35].

Another structural method of investigating fibres is small-angle X-ray scattering (SAXS). Uniaxially drawn fibres normally show a two-spot pattern indicating the presence of a lamellar structure aligned in columns. As the draw ratio and Young's modulus increases in PE the intensity of this SAXS pattern decreases, although the peak position (long spacing or crystal-thickness repeat distance) does not change much. The same type of pattern was obtained from the drawn gel fibres of PVA, and the long spacing remains in the range of 11 to 13 nm for all draw ratios. This is close to the range of long spacing that has been seen for PVA single crystals [41]. Only drawing at extremely high temperature has an effect on the long spacing. A 6.2% D-gel was drawn to $\lambda = 12.2$ at 180° C and its long spacing increased from 11 to 15 nm.

An important feature of fibre drawing is the extension of the entanglement network, so the crystal size and orientation as determined by X-ray diffraction is not as important as the molecular or network extension, M. Shrinkage of the drawn sample back to an isotropic relaxed state is the primary indication of molecular extension [42 – 44]. M is defined as (drawn length)/(shrunk length), L_d/L_s [33]. The shrinkage data were used to derive M and the retraction R described in Section 2.2, which is convenient for

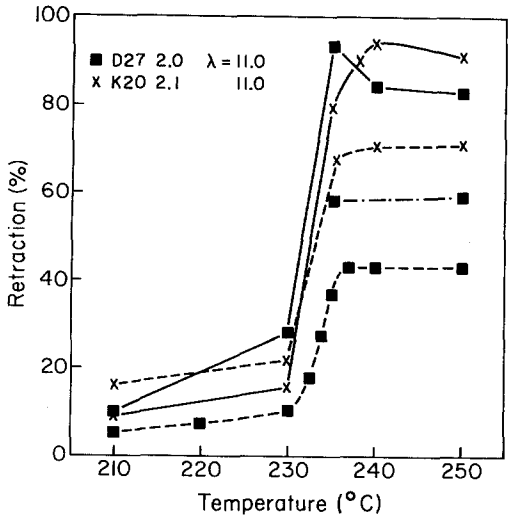

Figure 7 Retraction plotted as a function of temperature for fibres having a draw ratio $\lambda = 11.0$. Solid lines connect data points from separate specimens cut from one fibre. Dashed lines connect data points from a single specimen tested by slow heating through the full temperature range.

the comparison of samples of different draw ratios. Retraction and molecular extension are related by

$$M = \frac{1}{1 - R(1 - 1/\lambda)}$$

The calculations of molecular extension depend on the fibre retracting without competing relaxation of the extension. When fibres of the same draw ratio were subjected to different heating programmes, the measured retraction varied considerably as shown in Fig. 7. Solid lines in Fig. 7 connect data from the fast-heating test, where each point comes from a different small sample heated directly to the test temperature. The dashed lines connect data from slow-heating tests, where one sample was heated continuously and slowly. Irregularities in retraction at high temperatures, such as reduced retraction for temperatures above the melting point, are present only in the fast-heating tests. Absolute retractions, however, are much lower in the slow-heating tests. This indicates that the slow heating allows some relaxation of the oriented molecules. This hypothesis was tested by heating one sample, D27 in Fig. 7, continuously to the melting point, but at a much faster rate than used for the slow-heating tests. This did not allow many measurements of length to be made, but at the melting point the retraction is higher than that of the slow test and lower than that of the fast test. As retraction thus depends on heating rate, the fastest rate should be used, and the observed retraction is still only a lower limit, since with even faster rates, greater retractions might be achieved.

All fibres retract over a narrow range of temperature, and the great part of the observed retraction is over when the temperature reaches the melting point as found by thermal analysis. This gives some confidence that the measured melting points were of the freely retracting fibres, not strongly affected by constraints. Gels drawn from fibre starting material do continue to retract above the melting point, so that the maximum retraction may be seen at 250° C. The spread of retraction is consistent with the spread in the melting endotherm seen in these materials.

Table IV summarizes the retraction measured for a range of drawn samples, and the molecular extension M derived from R. The table also includes M/λ, a measure of the efficiency of molecular extension. (This was called R'' in

TABLE IV Retraction and molecular extension of gels

Sample	Concentration (%)	λ	T_d (° C)	R	M	M/λ
F1	9.3	11.0	145	0.92	6.1	0.55
D27	2.0	13.6	155	0.92	6.8	0.50
		12.4	145	0.892	5.5	0.44
		11.0	152	0.93	6.5	0.59
D14	2.0	6.0	147	0.91	4.1	0.69
C17	3.8	12.0	140	0.901	5.7	0.48
		6.3	151	0.897	4.1	0.65
C20	2.1	11.0	146	0.936	6.7	0.61
L5	2.4	12.2	148	0.96	8.4	0.69
L3	2.1	14	163	0.999	13.6	0.97
		12.2	163	0.923	6.5	0.54

Grubb [33].) The error in M is about M times the error in R, so that small errors in measurement of the final length after shrinkage can be serious. There are no clear trends of retraction or drawing efficiency with draw ratio, sample type or drawing temperature above 100° C. All of the samples drawn at high temperature (except possibly the first in Table IV) show drawing efficiencies M/λ of 40 to 70%. It is probable that the particular values found depend upon experimental conditions, primarily the heating rate but also the sample size due to constraint and surface-tension effects.

4. Conclusions

Coherent and homogeneous gels of PVA can be made from ethylene glycol/water solutions at concentrations above the overlap concentration c^*. When partially dried these gels can be drawn in the temperature range 140° to 160° C, with effective molecular extension to draw ratios of up to 14. This is a much larger extension than can be achieved by hot drawing of the melt-crystallized material, but a higher draw ratio of 19 has been obtained by zone drawing at 240° C. Structural studies show an improvement in crystallinity and in crystal perfection on drawing. At draw ratios of 10 to 14 the crystalline orientation is still improving with λ and there is still a strong SAXS peak indicating the presence of lamellar structures. The Young's modulus increases with draw ratio and the absolute values are quite close to those of PE at the same draw ratio, measured under the same conditions. The modulus of the most highly drawn fibres, 15 to 20 GPa, is high by normal polymer standards and close to that of commercial PVA fibres. All indications are that a further increase in draw ratio will produce an increase in Young's modulus.

Acknowledgements

The financial support of the Office of Naval Research is gratefully acknowledged. The authors are also indebted to the Kuraray Corporation and Dr P. Lemstra for the supply of material, and to Dr Lemstra and Dr P. Smith for helpful comments.

References

1. F. C. FRANK, *Proc. R. Soc.* **A319** (1970) 127.
2. H. TADOKORO, *Makromol. Chem. Suppl.* **2** (1979) 155.
3. T. OHTA, *Polym. Eng. Sci.* **23** (1983) 697.
4. G. CAPACCIO and I. M. WARD, *Polymer* **15** (1974) 233.
5. P. J. BARHAM and A. KELLER, *J. Mater. Sci.* **11** (1976) 27.
6. G. CAPACCIO, T. A. CROMPTON and I. M. WARD, *J. Polym. Sci., Polym. Phys. Edn.* **14** (1976) 1461.
7. A. ZWIJNENBURG and A. J. PENNINGS, *Colloid Polym. Sci.* **254** (1976) 868.
8. M. J. HILL, P. J. BARHAM and A. KELLER, *ibid.* **258** (1980) 899.
9. J. C. M. TORFS and A. J. PENNINGS, *J. Appl. Polym. Sci.* **26** (1981) 303.
10. P. SMITH, P. J. LEMSTRA, B. KALB and A. J. PENNINGS, *Polym. Bull.* **1** (1979) 733.
11. P. SMITH and P. J. LEMSTRA, *Colloid Polym. Sci.* **258** (1980) 891.
12. B. KALB and A. J. PENNINGS, *J. Mater. Sci.* **15** (1980) 1584.
13. P. SMITH, P. J. LEMSTRA and H. BOOIJ, *J. Polym. Sci., Polym. Phys. Edn.* **19** (1981) 877.
14. European Patent Application No. 82102964.2 (1982).
15. P. J. BARHAM, *Polymer* **23** (1982) 1112.
16. P. F. VAN HUTTEN, C. E. KONING, J. SMOOK and A. J. PENNINGS, *Polymer Commun.* **24** (1983) 237.
17. K. FURUHATA, T. YOKOKAWA and K. MIYASAKA, *J. Polym. Sci., Polym. Phys. Edn.* **22** (1984) 133.
18. G. HADZIIONIDES, private communication.
19. D. T. GRUBB, *J. Polym. Sci., Polym. Phys. Edn.* **21** (1983) 165.
20. A. PEGUY and R. ST. J. MANLEY, *Polymer Commun.* **25** (1984) 39.
21. C. G. CANNON, *Polymer* **23** (1982) 1123.
22. I. SAKURADA, T. ITO and K. NAKAMAE, *J. Polym. Sci. C* **15** (1966) 75.
23. L. Z. ROGOVINA, G. L. SLONIMSKII, L. S. GEMBITSKII, YE. A. SEROVA, V. A. GRIGOR'EVA and YE. N. GUBENKOVA, *Vysokomol. Soyed. A* **15** (1973) 1256.
24. E. PINES and W. PRINS, *Macromolecules* **6** (1973) 888.
25. V. M. ANDREYEVA, A. A. ANIKEYEVA, B. I. LIROVA and A. A. TAGER, *Vysokomol. Soyed. A* **15** (1973) 1770.
26. H. HALBOTH and G. REHAGE, *Angew. Makromol. Chem.* **38** (1974) 111.
27. S. MATSUZAWA, K. YAMAURA and H. KOBAYASHI, *Rep. Prog. Polym. Phys. Jpn.* **23** (1980) 39.
28. K. OGASAWARA, T. NAKAJIMA, K. YAMAURA and S. MATSUZAWA, *Prog. Colloid Polym. Sci.* **58** (1975) 145.
29. *Idem, Colloid Polym. Sci.* **254** (1976) 553.
30. K. YAMAURA, S. MATSUZAWA and Y. GO, *Kolloid-Z. u Z. Polymere* **240** (1971) 820.
31. Y. D. KWON, S. KAVESH and D. C. PREVORSEK, US Patent 4 440 711 (1984).
32. J. G. PRITCHARD, "Poly(vinyl alcohol): Basic Properties and Uses" (Gordon and Breach, London, 1970).

33. D. T. GRUBB, *J. Mater. Sci. Lett.* **3** (1984) 499.
34. P. SMITH and P. J. LEMSTRA, *Polymer* **21** (1980) 1341.
35. J. SMOOK, J. C. M. TORFS and A. J. PENNINGS, *Macromol. Chem.* **182** (1981) 3351.
36. S. N. ZHURKOV, B. YA. LEVIN and A. V. SAVITSKII, *Dokl. Akad. Nauk SSSR* **186** (1969) 132.
37. A. V. SAVITSKII, B. YA. LEVIN and V. P. DEMICHEVA, *Vysokomol. Soed. A* **15** (1973) 1286.
38. T. KUNUGI, A. SUZUKI and M. HASHIMOTO, *J. Appl. Polym. Sci.* **26** (1981) 1951.
39. R. S. PORTER, *Polym. Prepr. Amer. Chem. Soc., Div. Polym. Chem.* **12** (1971) 2.
40. P. J. BARHAM and R. G. C. ARRIDGE, *J. Polym. Sci., Polym. Phys. Edn.* **15** (1977) 1177.
41. J. F. KENNY and V. F. HOLLAND, *J. Polym. Sci. A1* **4** (1966) 699.
42. P. J. FLORY, *J. Amer. Chem. Soc.* **78** (1956) 5222.
43. A. M. RIJKE and L. MANDELKERN, *J. Polym. Sci. A2* **8** (1970) 225.
44. K. YAMADA, M. KAMEZAWA and M. TAKAYANAGI, *J. Appl. Polym. Sci.* **26** (1981) 49.

Received 28 December 1984
and accepted 16 January 1985